

# Spectropolarimetry of umbral fine structures from Hinode: Evidence for magnetoconvection

Lokesh Bharti<sup>1\*</sup> †, Chandan Joshi<sup>1</sup>, S.N.A. Jaaffrey<sup>1</sup> and Rajmal Jain<sup>2</sup>

*1. Department of Physics, University College of Science, Mohanlal Sukhadia University, Udaipur, 313001, India*

*2. Physical Research Laboratory, (Department of Space, Government of India) Navrangpura, Ahmedabad 380 009, India*

3 February 2022

## ABSTRACT

We present spectropolarimetric analysis of umbral dots and a light bridge fragment that show dark lanes in G-band images. Umbral dots show upflow as well as associated positive Stokes  $V$  area asymmetry in their central parts. Larger umbral dots show down flow patches in their surrounding parts that are associated with negative Stokes  $V$  area asymmetry. Umbral dots show weaker magnetic field in central part and higher magnetic field in peripheral area. Umbral fine structures are much better visible in total circularly polarized light than in continuum intensity. Umbral dots show a temperature deficit above dark lanes. The magnetic field inclination show a cusp structure above umbral dots and a light bridge fragment. We compare our observational findings with 3D magnetohydrodynamic simulations.

**Key words:** Sun: photosphere–Sun: magnetic fields–Sun: granulation - sunspots

## 1 INTRODUCTION

Two models of the umbral dots (UDs) are under discussion these days. The first is the cluster model (Parker, 1976 and Choudhuri, 1986), that suggests that UD are the top of the intrusion of field free material between the flux tubes beneath the sunspot. The second model is known as the monolithic model (Weiss, 2002 and reference therein) and suggest that UD show up because of magnetoconvection in monolithic flux tube. Recent simulations by Schüssler and Vögler (2006) with gray radiative transfer show UD appearing due to magnetoconvection in strong background magnetic field. Knowledge of the nature of UD is essential to understand the energy transport from below the sunspot (see reviews from Solanki, 2003 and Thomas & Weiss, 2004 and reference therein on the subject).

Bharti *et al.* (2007a) analyzed Dopplergrams obtained from filtergraph data and they found a correlation between intensity and velocity in UD, which suggests a magnetoconvective origin. Using high quality G-band images from Hinode, Bharti *et al.* 2007b reported on dark lanes in UD. These separate observational findings are compatible with some aspects of simulations by Schüssler and Vögler (2006). Socas-Navarro *et al.* (2004) analysed peripheral UD in detail from spectropolarimetric data and find higher tempera-

ture ( $\sim 1$  kK), weaker field ( $\sim 500$  G), small upflow ( $\sim 100$  m<sup>-1</sup>) and more inclined field ( $\sim 10^\circ$ ) in UD.

In this article we present spectropolarimetric analysis of dark laned umbral fine structure from Hinode spectropolarimetric data. The high polarimetric sensitivity and spatial resolution achieved by Hinode spectropolarimeter now it became possible to compare observational results directly with predictions of numerical simulations (Rezaei *et al.*, 2007, Sainz Dalda and Bellot Rubio, 2008).

## 2 OBSERVATIONS AND INVERSION TECHNIQUE

We used spectropolarimetric data obtained by the spectropolarimeter onboard the Hinode (Kosugi *et al.*, 2007) on December 12, 2006. The four Stokes profiles of the two iron line pairs at 630.15 nm (Lande factor  $g=1.67$ ) and 630.25 nm ( $g=2.5$ ) were recorded for the active region 10930 close to the disk center ( $\mu=0.99$ ). We used fast map. The integration time for fast map was 3.2 sec. The field of view comprises an area of  $295'' \times 162''$ . The spatial sampling for the fast map was  $0''.316$  along the slit and  $0''.295$  in the scanning direction. The spatial resolution of the resulting spectropolarimetric map is approximately  $0''.6$  for the fast map with the spectral sampling at 2.15 pm. The calibration of the SP data is described by Ichimoto *et al.* (2007). We used the Solar-Soft pipeline to calibrate the SP data.

To derive accurate photospheric height stratification of

\* E-mail: lokesh\_bharti@yahoo.co.in

† Currently at Max-Planck Institute for Solar System Research, 37191 Katlenburg-Lindau, Germany

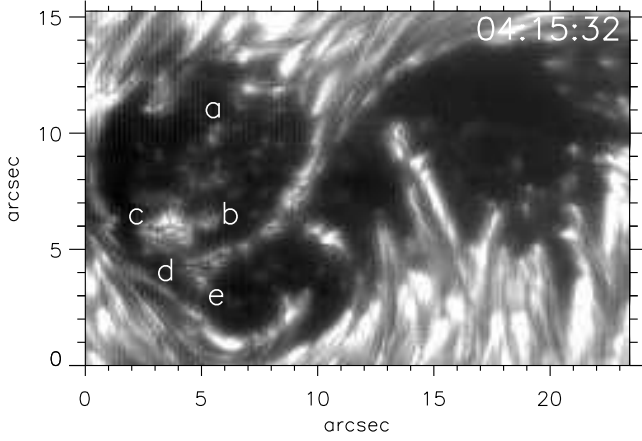


**Figure 1.** A G-band image as observed in the broad-band filter on SOT at 04:15:32 UT. The image is byte-scaled and shows the fine structure of the sunspot around the time that our spectropolarimetric maps were taken.

the temperature ( $T$ ), magnetic field strength ( $B$ ), line of sight velocity ( $V_{los}$ ), and inclination ( $\gamma$ ), we employ the SIR code (Ruiz Cobo and Del Toro Iniesta 1992). This code presumes hydrostatic equilibrium and local thermodynamic equilibrium (LTE). By solving numerically the radiative transfer (RTE) equation for polarized light the inversion code SIR computes the synthetic Stokes profiles. The optimal parameters for the model were determined iteratively. The difference between the observed and synthetic Stokes profiles was minimized using a non-linear, least square Marquardt's algorithm. The values of the physical parameters are computed at only a few grid points called nodes instead of computing at all optical depths of the model. For rest of depths, they are approximately computed by the cubic-spline interpolation between the equidistantly distributed grid points. We perform the SIR inversion with only one magnetic component, for which we allow 5 nodes in  $T(\tau)$ , 3 for  $B(\tau)$ ,  $V_{los}(\tau)$ , and  $\gamma(\tau)$ .

G-band time series obtained in the broadband filter were used to follow the evolution of the sunspot fine structure as seen in the SP maps (see Bharti *et al.*, 2007b). Wiener filtering was applied to the G-band images for the point spread function correction of telescope. Understanding of the evolution of the umbral fine structure is necessary as they may have common physical origin (Rimmele 2008, Katsukawa *et al.* 2007). Here we would like to mention that it is our aim to investigate dark lane in UD as reported by Bharti *et al.* (2007b) and the SP fast scan at 0.6 spatial resolution cover similar features.

The calibrated Stokes profiles were used to create maps of total circular polarization (TCP) and Stokes  $V$  area asymmetry (Bellot Rubio *et al.*, 2007).

### 3 RESULTS

We have chosen G-band images, whose timing was close to the SP scans. Figure 1 shows one of the G-band images taken close to the fast SP scan time at 04:15:32 UT that cover emerging sunspot in the SP map. The G-band time series shows UD 'a' has been forms from a peripheral um-

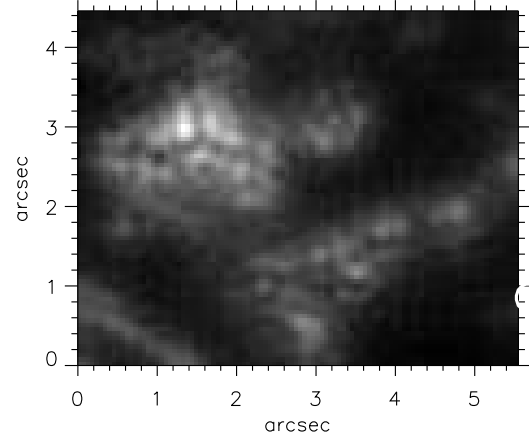


**Figure 2.** Enlarged view of an area of Figure 1. It clearly shows dark lanes inside the umbral fine structure.

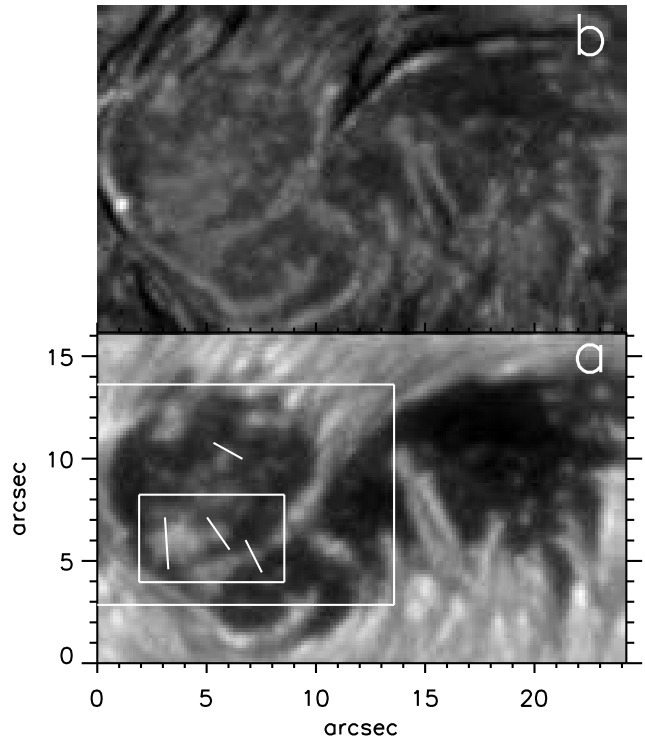


**Figure 3.** Maps showing continuum intensity (a) and total circular polarization (b) for the emerging sunspot that rises below a developed sunspot in AR 10930. Marked in white in panel (a) are the location where stratifications of various physical parameters along cut were measured. All maps are up scaled two times using cubic spline interpolation. The outer rectangle shows the field of view that was subjected to the SIR inversion and the inner rectangle shows the region that was subjected to area asymmetry measurement.

bral dot (PUD) that fragmented in two UDs. The UD 'b' emerges from a bright bands (Bharti *et al.*, 2007b). The bright band fragments and a UD forms, it grows gradually and shows a threefold dark lane. At 04:15:32 UT it shows a central bright structure surrounded by a dark ring and five fragments separated by dark lanes. The time series show that this UD fragments and again converts in to a bright

band. A larger UD ‘c’ forms from a bright band that show complex shapes during its evolution. In Figure 1 it shows clearly threefold dark lanes. The light bridge that develops from the dark cored penumbral filament shows central dark lanes and its fragments show dark lanes. At the head of the light bridge a triangular shaped bright structure ‘d’ is seen that forms from the light bridge fragments in upper part and conglomeration of an UD that appears from the diffuse background. This UD is marked by ‘e’. Individual UDs are seen. However, their boundary is not clearly visible. Close to the vertex of the triangular structure ‘d’ a light bridge fragment is seen that shows dark lane. Dark lanes in UDs and light bridge fragments are visible but only UD ‘c’ shows more clearly dark lane in the G-band image. Figure 2 shows enlarged view of a part of Figure 1 that shows dark lanes in umbral fine structures very clearly.

Figure 3 illustrates map of the emerging sunspot taken from the SP fast scan. Panel (a) of Figure 3 shows the continuum intensity map; the fine structure is very similar to that of the G-band image. Comparison with the G-band image in Figure 1 illustrates that it is reasonable to analyse these fine structures using the spectropolarimetric fast scan at 0//.6 resolution. However, the UD marked by an ‘a’ in Figure 1 shows clear structure in this figure, but not at the lower resolution in Figure 3. The light bridge fragments are visible in the continuum image of the SP map (Figure 3(a)). Figure 3(b) depicts TCP map of the same emerging sunspot. One can see that umbral fine structure such as UDs and diffuse background are much more prominent in the polarized light than in the continuum intensity. Appearance of umbral fine structure more prominently in the polarized light suggests that there is no one to one relationship between the umbral continuum intensity signatures and umbral magnetic fields. Hence, the umbral inhomogeneities can not be completely characterized only based on the intensity measurement of umbral fine structures and should be treated cautiously. Similar conclusion was drawn by Bellot Rubio *et al.* (2007) for dark cored penumbral filament from the SP normal map at 0//.3 resolution. This also helps us to find dark nuclei for zero velocity reference.

Figure 4 shows the height stratification of plasma parameters according the SIR inversion. This Figure shows temperature ( $T(\tau)$ ), magnetic field strength ( $B(\tau)$ ), line-of-sight velocity ( $V_{los}(\tau)$ ) and inclination ( $\gamma(\tau)$ ) as a function of altitude and horizontal distance across the lines in panel (a) of Figure 3 for umbral fine structures for optical depths  $0 < \log(\tau) < 2.5$ . We find these parameters reliable for  $\log(\tau) < -2.0$ ; i.e. error are higher in the upper atmosphere. From the top downwards, the plot shows umbral dots ‘a’, ‘b’, ‘c’ and the light bridge fragment.

The first column of Figure 4 illustrates the temperature stratification of the observed UDs and the light bridge fragment. At  $\tau=1$ , UDs ‘a’, ‘b’, ‘c’ and the light bridge fragment are 780 K, 810 K, 1220 K and 870 K respectively hotter than the coolest part of the sunspot. This is in agreement with Sobotka and Hanslmeier (2005) who reported from two color photometry, on average, UDs are about 1000 K hotter from the coolest area in the umbra. In all cases these structures are cooler in the higher layers. In case of UD ‘c’ a temperature drop can be seen around  $\log(\tau) = -1.5$ , which is colocated with dark lane. This dark lane has higher contrast in the line core of the 630.25 nm line as shown by the dotted

line overplot in Figure 4. However, as shown by the solid line overplot in Figure 4 this dark lane is not visible in the continuum of the 630.25 nm line. This indicates that dark lanes have lower temperature compared to the surrounding at the same optical depth. This is in agreement with Schüssler and Vögler (2006) and Spruit and Scharmer (2006). They suggest that the surfaces of constant optical depths are elevated in these structures, so that they correspond to lower temperature. This dark lane can be produced by the effect of the density and the gas pressure. The SIR code takes those into account only approximately under the approximation of hydrostatic equilibrium. Ruiz Cobo and Bellot Rubio (2008) modeled dark lanes in penumbral filaments and suggested dark lanes are produced by locally enhanced density and pressure that shift the  $\tau=1$  level to higher layers. All three thermodynamic parameters (temperature, density and gas pressure) are likely to play a role, as suggested by Borrero (2007). The dark lane is identified clearly in the temperature map at higher layers (not shown here), which consistent with a elevated  $\tau=1$  level lies above UD in the higher layers. We find a temperature variation in the UD ‘c’, which suggests that multifold dark lanes are the manifestation of a temperature deficit. To our knowledge this is the first observational evidence of temperature deficit in dark lanes of UDs.

The second column of Figure 4 shows the magnetic field strength stratification of these structures. The field strength in UDs decreases rapidly with depth. On the other hand, background field strength increases slightly. We find there is a strong difference between the values in the central part and the peripheral part of UDs. The magnetic field is less in the central part and higher in the peripheral parts. At  $\tau=1$  level, with respect to the dark nuclei this difference is found to be 441 G, 440 G, 900 G and 325 G for UD ‘a’, ‘b’, ‘c’ and the light bridge fragment, respectively. This is in agreement with findings of Schüssler and Vögler (2006). We find higher magnetic field in the peripheral part of these structures. Joshi *et al.* (2007) reported similar trend in and around UDs in their analytical study on the Joule heating in UDs that suggests the higher magnetic field in the peripheral part of UDs.

The line-of-sight velocity stratification for these umbral fine structures is shown in the third column of Figure 4. UD ‘a’, ‘b’ and ‘c’ show upflow of 300, 280 and 450  $\text{ms}^{-1}$ , respectively with associated downflow at edges. The light bridge fragment shows upflow in the middle and downflow at the right edge.

The fourth column of Figure 4 depicts the inclination stratification for these UDs and the light bridge fragment. We can see more inclined field above these structures. At  $\tau=1$  the field is inclined around  $10^\circ$  for UDs ‘a’ and ‘b’ and the light bridge fragment. However, field is strongly inclined for UD ‘c’, up to  $20^\circ$  at  $\tau=1$ . Such inclined fields forms a cusp above these structures. Cusp above UDs predicted by Schüssler and Vögler (2006) in the simulations. Borrero *et al.* (2008) reported magnetic field wrapping around penumbral filaments. This is consistent with field geometry we observed for UDs.

Shown in Figure 5 is the line of sight velocity map of region of interest shown by outer rectangle in Figure 1 for the fast scan at  $\log(\tau) = -1.5$ . The UD ‘c’ shows upward velocity up to 450  $\text{ms}^{-1}$ . On the other hand other UDs show upflow

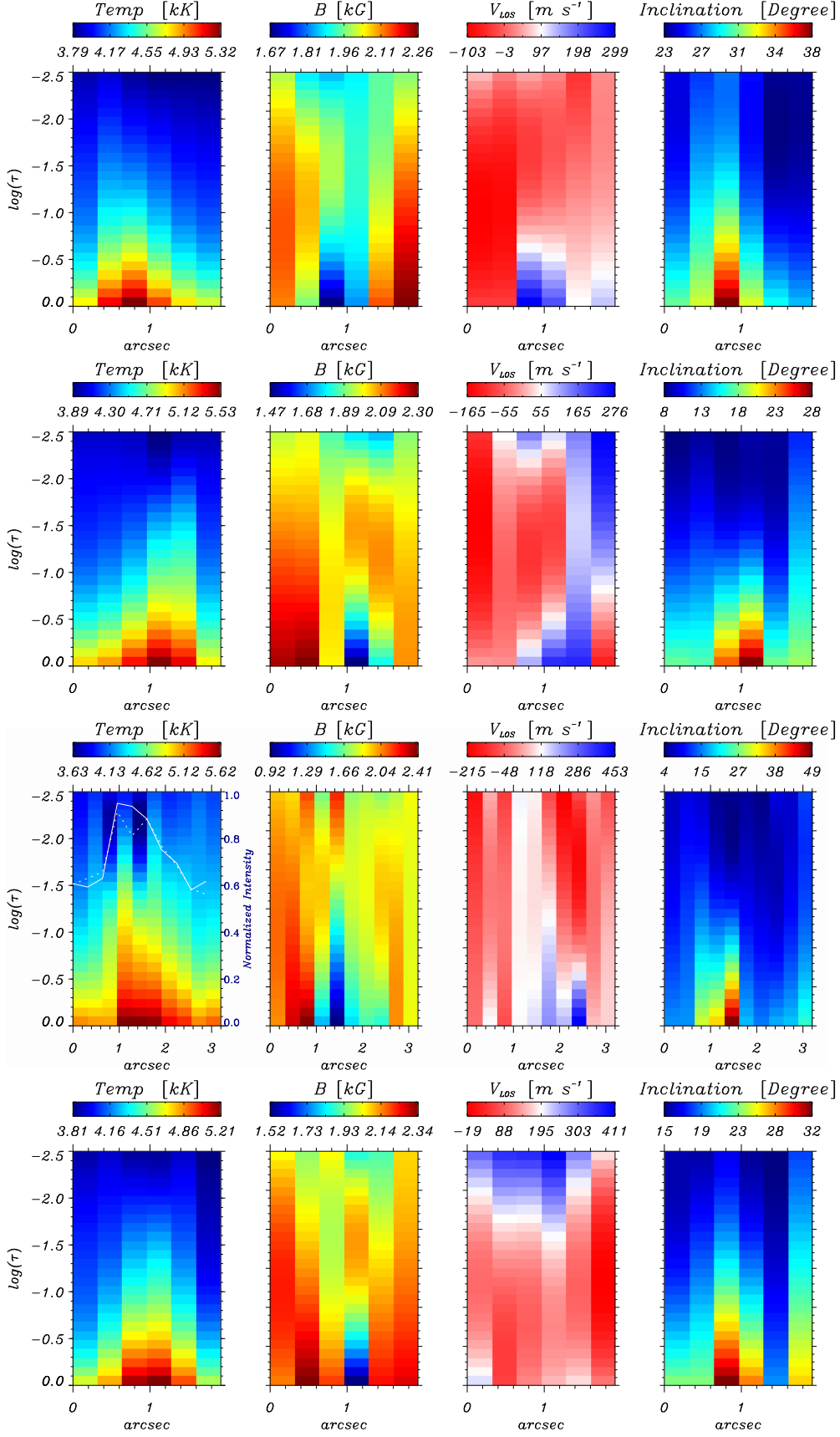


**Figure 4.** From left to right: temperature, magnetic field strength, LOS velocity and inclination. From top to bottom: UD's a, b, c and light bridge. For UD 'c' continuum (solid line) and core intensity (dotted line) overplotted. Positive velocity corresponds to upflow and negative velocity to downflow.

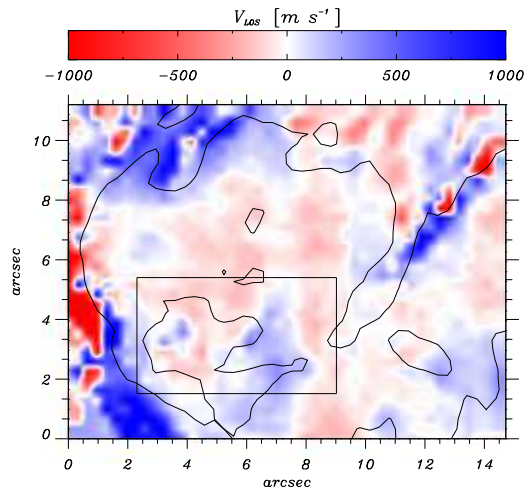


**Figure 5.** LOS velocity map derived from inversion for fast scan at  $\log(\tau) = -1.5$ . UDs show upflow. Bigger UD ‘C’ as shown in Figure 1 show upflow in central part and downflow patches around it. Velocity scaled between  $\pm 1000 \text{ ms}^{-1}$ . Blue show upflow and red show downflow. Contour of continuum intensity is overplotted. Rectangle show location of region of interest subjected to area asymmetry measurement.

of the order of  $300 \text{ ms}^{-1}$  which is in agreement with finding of Socas-Navarro *et al.* (2004) and Bharti *et al.* (2007a). However we observed down flow patches around larger UD ‘c’. This is in agreement with Bharti *et al.* (2007a) who reported downflow around UDs. However, we haven’t observed downflow around smaller UDs. That may be due to the lower spatial resolution in analysed data for present study. Upward velocity in the central parts and downflow around the peripheral parts of UDs suggest their magnetoconvective origin as reported by Schüssler and Vögler (2006). Since this sunspot was located close to the disk center hence the line of sight component of the velocity is assumed to be vertical.

Shown in Figure 6 (right) is enlarged Stokes  $V$  area asymmetry map of selected UDs in Figure 3(a). Contours of continuum intensity image (left) are plotted over area asymmetry map (right). On comparing with rectangular region in velocity map in Figure 5, one can see that upflow region of UD ‘c’ shows positive area asymmetry whereas downflow patches around this UD show negative area asymmetry. Similar trend can be observed for UDs in a triangular region ‘d’ and the light bridge fragment. UD ‘b’ shows very interesting pattern of area asymmetry, as shown in Figure 2. It shows bright ring with dark lanes around a bright UD. We can see this ring as positive area asymmetry signature with lesser positive area asymmetry in the center, producing a donut-shaped structure. Auer and Heasley (1978) suggested that to produce an area asymmetry  $\delta A$ , a gradient in the velocity is required. On the other hand, a combination of gradients in the field strength or orientation and velocity can produce an asymmetry in much more efficient manner. We observed positive area asymmetry in the upflow region and negative area asymmetry at the downflow region of UDs, however only brighter UDs show up positive area asymmetry above background noise.

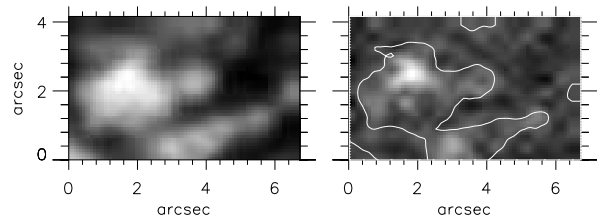


**Figure 6.** Enlarged view of continuum image of UDs and light bridge fragments (left). Enlarged view of area asymmetry map of UDs and light bridge fragments (right), contour of continuum intensity from left image is overplotted. UDs and light bridge fragments clearly show positive area asymmetry in central part of these structures.

## 4 DISCUSSION AND CONCLUSIONS

In this study we present a spectropolarimetric analysis using sophisticated inversion technique of umbral fine structure that shows dark lanes in G-band images. Seeing free data from *Hinode* with high spatial resolution of at  $0.6$  resolution enables us to study stratification of various parameters associated with umbral fine structure.

Our results support several aspects of 3D MHD simulations with gray radiative transfer by Schüssler and Vögler (2006) such as dark lanes in umbral dots and the light bridge fragments, temperature deficit in dark lanes, higher LOS magnetic field at the periphery of UDs, magnetic field reduction in the central part of UDs, more inclined magnetic field around UDs, upflow in the central part of UDs and downflow in patches around larger UDs. These facts suggest that UDs appear as a result of magnetoconvection in strong background magnetic field in the sunspot umbra.

Schüssler and Vögler (2006) show that UDs have elongated shapes and that there is downflow associated at the end points of dark lanes. The spatial resolution of our observations is insufficient to confirm such flow pattern. We observed downflow patches around a larger UD, and a comparison with the dark lanes in the G-band image, suggests that downflows are not associated with dark lane end points. This larger UD may have different origin, as a result of flux separation (Weiss *et al.* 2002). Thus, granular-like convection similar to quiet regions appears in a large field-free patches. Hence we could observe downflows surrounded around overturning convective cells. However, the stratification of plasma parameters that we found for UD ‘c’, which displays several dark lanes, is compatible with results of Schüssler and Vögler (2006).

Riethmüller *et al.* (2008a) presented an analysis similar to ours of a large number of central and peripheral UDs. They used *Hinode* normal SP scan at a resolution of  $(0.3)$  and obtained results similar to ours. At the  $\log(\tau) = 0$  level they found that peripheral UDs on average exhibit a temperature enhancement of  $570 \text{ K}$ , a weaker magnetic field of  $510 \text{ G}$ , and upflow of  $800 \text{ ms}^{-1}$ . On the other hand, their central UDs on average display a  $550 \text{ K}$  higher temperature, a weaker field of  $480 \text{ G}$ , and no significant upflow signature. However, we find central UD ‘b’ and ‘c’ are hotter by  $810 \text{ K}$  and  $1221 \text{ K}$  respectively, show upflow of a few times  $100 \text{ ms}^{-1}$  and have a more inclined field ( $10^\circ$  and  $20^\circ$ , respectively). The downflows around the UDs reported by Rieth-

muller et al. (2008) are in good agreement with our present study and confirm the findings of Bharti *et al.* (2007a).

The asymmetry in the area that we studied suggests that there are gradients in the magnetic field, the upflow and downflow velocities, and in the inclination of the magnetic field. Sánchez Almida and Lites (1992) suggested the so-called  $\Delta\gamma$  mechanism, i.e. the simultaneous variation of the velocity and magnetic field inclination to explain area asymmetry. Solanki and Montavon (1993) showed sign dependence of an area asymmetry on combinations of gradients of these quantities. Equation (2) and (3) of Solanki and Montavon (1993) show the sign of the observed area asymmetry  $\delta A$  in and around UDs. These equations are given by:

$$\text{sign}(\delta A) = -\text{sign}\left(\frac{dV_{los}}{d\tau} \cdot \frac{d|B|}{d\tau}\right), \quad (1)$$

$$\text{sign}(\delta A) = -\text{sign}\left(\frac{dV_{los}}{d\tau} \cdot \frac{d|\cos\gamma|}{d\tau}\right). \quad (2)$$

Where  $V_{los} > 0$  for a velocity directed away from the observer.

The central part of UDs show:  $d|B|/d\tau < 0$ ,  $dV_{los}/d\tau > 0$ , and  $d|\cos\gamma|/d\tau < 0$ , thus implying positive area asymmetry. In the peripheral part we find:  $d|B|/d\tau > 0$ ,  $dV_{los}/d\tau > 0$ , and  $d|\cos\gamma|/d\tau > 0$  which implies negative area asymmetry. Thus, upflow regions show positive area asymmetry and downflow ones show negative area asymmetry. The gradient we found for these quantities and for the area asymmetry in and around UDs are compatible with the model suggested in Figure 2 of Schüssler and Vögler (2006). However, due to the limit set by the spatial resolution of our observations we can not observe such asymmetries around smaller UDs (i.e. narrow downflow channels concentrated at the end points of dark lanes). Schüssler and Vögler (2006) also suggested that line forming region above UDs lies in higher height, thus strong field reduction and high upflow velocities may not be observable in spectroscopic observation, this is in agreement with our findings.

Spectropolarimetry of UDs with the Narrowband Filter Imager (NFI) and Dopplergrams of the magnetically insensitive line 5576 Å at a 0.2 will be very useful for detailed studies of umbral fine structure. On the other hand, observations of umbral fine structure at different heights in solar atmosphere from ground based facilities will be our next aim.

## ACKNOWLEDGEMENTS

Juan Manuel Borrero, Jan Jurčák and Luis Bellot Rubio (who kindly provided SIR code) are gratefully acknowledged for discussion on SIR inversion. We thank Prof. Manfred Schüssler and Dr. Michal Sobotka for useful discussions. We indebted to an anonymous referee for useful suggestions to improve the presentation of this work. Dr. Nick Hoekzema and Dr. Ajay Manglik are gratefully acknowledged for help with language. Hinode is a Japanese mission developed and launched by ISAS/JAXA, with NAOJ as domestic partner and NASA and STFC (UK) as international partners. It is operated by these agencies in co-operation with ESA and NSC (Norway). This research is supported by Bal Shik-

sha Sadan Samiti (a nongovernmental organization [NGO] , Udaipur.)

## REFERENCES

- Auer, L. H. and Heasley, J. N.: 1978, *A&A*, 64, 67  
 Bellot Rubio, L. R., Tsuneta, S. and Ichimoto, K. et al.: 2007, *ApJ*, 668, L91  
 Bharti, L., Joshi, C. and Jaaffrey, S. N. A.: 2007a, *ApJ*, 669, L57  
 Bharti, L., Jain, R. and Jaaffrey, S. N. A.: 2007b, *ApJ*, 665, L79  
 Borrero, J. M.: 2007, *A&A*, 471, 967  
 Borrero, J. M.; Lites, B. W.; Solanki, S. K.: 2008, *A&A*, 481, L13  
 Choudhuri, A. R.: 1986, *ApJ*, 302, 809  
 Joshi, C., Bharti, L. and Jaaffrey, S. N. A.: 2007, *Solar Phys.*, 245, 239  
 Socas-Navarro, H., Martínez Pillet, V., Sobotka, M. and Vázquez, M.: 2004, *ApJ*, 614, 448  
 Spruit, H. C. and Scharmer, G. B.: 2006, *A&A*, 447, 343  
 Ichimoto, K., Lites, B. W., Elmore, D., et al.: 2007, *Solar Phys.*, 249, 233  
 Katsukawa, Y., Yokoyama, T., Berger, T. E., et al.: 2007, *PASJ*, 59, S577  
 Kosugi, T., et al.: 2007, *Solar Phys.*, 243, 3  
 Leka, K. D.: 1997, *ApJ*, 484, 900  
 Parker, E. N.: 1979, *ApJ*, 234, 333  
 Rezaei, R., Steiner, O., Wedemeyer - Böhm, S., Schlichenmaier, R., Schmidt, W. and Lites, B. W.: 2007, *A&A*, 476, L33  
 Riethmüller, T. L., Solanki, S. K. and Lagg, A.: 2008, *ApJ*, 678, L157  
 Riethmüller, T. L., Solanki, S. K., Zakharov V. and Gandorfer, A.: 2008, *A&A*, to be submitted  
 Rimmele, T.: 2008, *ApJ*, 672, 684  
 Ruiz Cobo, B. and Bellot Rubio, L. R.: 2008, *A&A*, 488, 749  
 Ruiz Cobo, B. and del Toro Iniesta, J. C.: 1992, *ApJ*, 398, 375  
 Sainz Dalda, A. and Bellot Rubio, L. R.: 2008, *A&A*, 481, L21  
 Sanchez Almeida and Lites, B. W.: 1992, *ApJ*, 398, 359  
 Schüssler M. and Vögler A.: 2006, *ApJ*, 641, L73  
 Sobotka, M. and Hanslmeier, A.: 2005, *A&A*, 442, 323  
 Solanki, S. K.: 2003, *Annu. Rev. Astron. Astrophys.*, 11, 153  
 Solanki, S. K. and Montavon, c. A. P.: 1993, *A&A*, 275, 283  
 Spruit, H. C. and Scharmer, G. B.: 2006, *A&A*, 447, 343  
 Thomas J. H. and Weiss N. W.: 2004, *Annu. Rev. Astron. Astrophys.* 2004, 42, 517  
 Tsuneta, S., et al.: 2007, *Solar Phys.*, 249, 167  
 Weiss N. O.: 2002, *Astron. Nachr.*, 323, 371  
 Weiss N. O., Proctor M. R. E. and Brownjohn D. P.: 2002, *MNRAS*, 337, 293

This paper has been typeset from a  $\text{\LaTeX}$  file prepared by the author.